

---

# A BASELINE FOR MACHINE-LEARNING-BASED HEPATOCELLULAR CARCINOMA DIAGNOSIS USING MULTI-MODAL CLINICAL DATA

---

A PREPRINT

**Binwu Wang    Isaac Rodriguez    Leon Breitinger    Fabian Tollens    Timo Itzel    Dennis Grimm**

**Andrei Sirazitdinov    Matthias Frölich    Stefan Schönberg    Andreas Teufel    Jürgen Hesser**

**Wenzhao Zhao** \*

## ABSTRACT

The objective of this paper is to provide a baseline for performing multi-modal data classification on a novel open multimodal dataset of hepatocellular carcinoma (HCC), which includes both image data (contrast-enhanced CT and MRI images) and tabular data (the clinical laboratory test data as well as case report forms). TNM staging is the classification task. Features from the vectorized preprocessed tabular data and radiomics features from contrast-enhanced CT and MRI images are collected. Feature selection is performed based on mutual information. An XGBoost classifier predicts the TNM staging and it shows a prediction accuracy of  $0.89 \pm 0.05$  and an AUC of  $0.93 \pm 0.03$ . The classifier shows that this high level of prediction accuracy can only be obtained by combining image and clinical laboratory data and therefore is a good example case where multi-model classification is mandatory to achieve accurate results.

**Keywords** Hepatocellular carcinoma · multi-modal clinical data · radiomics feature.

## 1 Introduction

Hepatocellular carcinoma (HCC) is one of the most common primary liver cancers and is associated with high cancer mortality Balogh et al. [2016]. The clinical diagnosis of HCC typically involves data from a variety of sources. Combining information from multiple sources is helpful for a more robust and accurate diagnosis.

Image data is an important source of information for HCC diagnosis Hennedige and Venkatesh [2013]. Dynamic multiphase contrast-enhanced CT and MRI are considered the current standard for imaging diagnosis of HCC. In addition to image data, tabular data such as clinical laboratory test data and case report forms are another important source of information. These data can be extracted from electronic health record systems. These data, collected over a long period of time, allow the physician to make a comprehensive assessment of the patient's status Abhyankar et al. [2012], Patridge and Bardyn [2018].

---

\*Binwu Wang is with Mannheim Institute for Intelligent Systems in Medicine, Medical Faculty Mannheim, Heidelberg University. Isaac Rodriguez, Leon Breitinger, Fabian Tollens, and Timo Itzel are with UMM Mannheim, Mannheim, Germany. Dennis Grimm is with Complex data processing in medical informatics (CMI), Mannheim Medical Faculty, Heidelberg University. Andrei Sirazitdinov is with Mannheim Institute for Intelligent Systems in Medicine, Medical Faculty Mannheim, Heidelberg University. Matthias Frölich and Stefan Schönberg are with Clinic for Radiology and Nuclear Medicine, Medical Faculty Mannheim, Heidelberg University, Mannheim, Germany. Andreas Teufel is with Heidelberg University, Mannheim, Germany. Jürgen Hesser is with Interdisciplinary Center for Scientific Computing, Central Institute for Computer Engineering, CSZ Heidelberg Center for Model-Based AI, Data Analysis and Modeling in Medicine, Mannheim Institute for Intelligent Systems in Medicine, Medical Faculty Mannheim, Heidelberg University. Wenzhao Zhao is with School of Information Engineering, Nanjing University of Finance and Economics and Interdisciplinary Center for Scientific Computing, Mannheim Institute for Intelligent Systems in Medicine, Medical Faculty Mannheim, Heidelberg University. E-mail: zhaowenzhaoyz@163.com.

Table 1: The patient distribution of the TNM stage labels of the QHCC dataset.

Labels	T0	T1	T2	T3	T4	TX	Null	Total
Number of Patients	1	53	22	13	5	1	5	100

In recent years, machine learning methods have received much attention and have shown great potential for improving cancer diagnosis. Most of the research works apply the machine learning methods only to image data or sometimes only to tabular dataXia et al. [2023]. Obviously, the limitation of the information source can affect the diagnosis performance. In this paper, we present a baseline for HCC diagnosis with both image data and tabular data.

## 2 Materials and Methods

### 2.1 QHCC dataset

The QHCC dataset consists of clinical data collected from 100 patients with HCC. The clinical data include CT, MRI, clinical laboratory test reports (see appendix), and research electronic data capture (REDCap)Patridge and Bardyn [2018] case report forms collected before and after hepatectomy. The lesions in both the venous and arterial phases of 179 contrast-enhanced T1w MRI and 127 contrast-enhanced CT images are segmented by a medical professional.

In this paper, we consider TNM stagingSubramaniam et al. [2013] as the classification task. 95 patients with TNM staging labels are selected. For the training and validation of the machine learning model, five rounds of patient-level random permutation cross-validation are performed, where the training and test sets are assigned at a ratio of 4 : 1.

The tabular data consists of multiple columns with each column corresponding to a variable. The procedure of filtering or selecting columns of Redcap data is detailed in Appendix A. The information of the selected variables for the lab data is shown in Appendix B.

### 2.2 Data preprocessing

For the tabular data, the non-numerical elements are converted to numerical labels. The missing values are replaced using a mean value for each variable.

As for the target prediction label, we observe that the distribution of the T-stage labels is highly unbalanced as shown in Table 1. To better balance the label distribution, we merge the labels "T0", "T1", and "TX" into the label "TX, T0 or T1", and "T3" and "T4" into the label "T3 or T4".

As each patient has multiple contrast-enhanced MRI and CT images, we augment the data using different combinations of MRI and CTs with the Redcap and Lab data. In this way, we get 376 samples, each consisting of an MRI image, a CT image, and the corresponding Redcap and lab data.

### 2.3 Radiomics feature extraction

The largest lesions in contrast-enhanced MRI and CT images are considered. We use PyRadiomicsVan Griethuysen et al. [2017] to extract the radiomics features from the segmented lesions. The radiomics feature classes considered include shape-based first-order statistics (3D), gray level co-occurrence matrix (GLCM), gray level run length matrix (GLRLM), gray level size zone matrix (GLSZM), gray level dependence matrix (GLDM), and neighboring gray tone difference matrix (NGTDM).

### 2.4 Feature selection

We select related features from the preprocessed tabular data and the extracted radiomics features based on the training set. The mutual informationShannon [1948] for the discrete target variable is estimated using Sklearn functionsPedregosa et al. [2011]. At least half of the features are selected to build the input vectors for the machine learning classifier. We adopt the methods of recursive feature elimination with cross-validationGuyon et al. [2002] to determine the number of features to be selected for the given training samples.

Table 2: The classification results on the QHCC dataset.

	Redcap data		Lab data		Redcap + Lab data		Null	
	ACC	AUC	ACC	AUC	ACC	AUC	ACC	AUC
CT	$0.88 \pm 0.04$	$0.90 \pm 0.06$	$0.51 \pm 0.08$	$0.68 \pm 0.08$	$0.83 \pm 0.07$	$0.90 \pm 0.02$	$0.55 \pm 0.08$	$0.64 \pm 0.06$
MRI	$0.83 \pm 0.12$	$0.88 \pm 0.09$	$0.49 \pm 0.06$	$0.65 \pm 0.10$	$0.89 \pm 0.05$	$0.93 \pm 0.03$	$0.51 \pm 0.10$	$0.57 \pm 0.08$
CT + MRI	$0.88 \pm 0.05$	$0.90 \pm 0.07$	$0.55 \pm 0.04$	$0.69 \pm 0.09$	$0.86 \pm 0.03$	$0.92 \pm 0.02$	$0.54 \pm 0.09$	$0.60 \pm 0.03$
Null	$0.82 \pm 0.12$	$0.88 \pm 0.12$	$0.48 \pm 0.06$	$0.50 \pm 0.06$	$0.85 \pm 0.07$	$0.90 \pm 0.04$	Null	Null

## 2.5 Classifier training and test

We adopt XGBoostChen and Guestrin [2016] as the classifier, which is one of the most efficient gradient-boosted decision trees (GBDTs) and also the state-of-the-art machine learning method for tabular dataMcElfresh et al. [2024]. We use the softmax objective. The evaluation loss is the cross-entropy loss for multi-class.

## 3 Results

We consider two metrics: the prediction accuracy (ACC) and the area under the curve (AUC). The "mean  $\pm$  std" is reported. Table 2 shows the ACC and AUC results for inputs of different combinations. It shows that Redcap data allows for higher prediction accuracy than other data. Adding lab data can improve the performance further. Both the radiomics features extracted from CT and MRI can help to improve the prediction based on Redcap data or lab data. CT radiomics features work better with Redcap data for prediction. The higher classification accuracy is achieved by combining MR radiomics features with Redcap and lab data. When using all the tabular data and radiomics features, we get the smallest prediction std with the second-best AUC score.

Fig. 1 shows the importance of selected tabular features considering the experiment with a random seed using only Redcap and lab data. Fig. 2 shows the importance of radiomics features when doing prediction with only radiomics features.

Fig. 3 shows the probability distributions of the predictions as well as the corresponding one-vs-rest receiver operating characteristic (ROC) curves for experiments with all the data modalities.

From the results, we can see that the tabular data-only or the radiomics-feature-only prediction may not give a favorable prediction accuracy. The radiomics features related to the tumor size and shape, the age of the patients, and "Tumor value" variable in the tabular data are frequently selected as highly related features for TNM staging, which is reasonable and is demonstrated from the feature importance shown in Fig. 1. The combination of both tabular data and radiomics features gives the highest prediction performance.

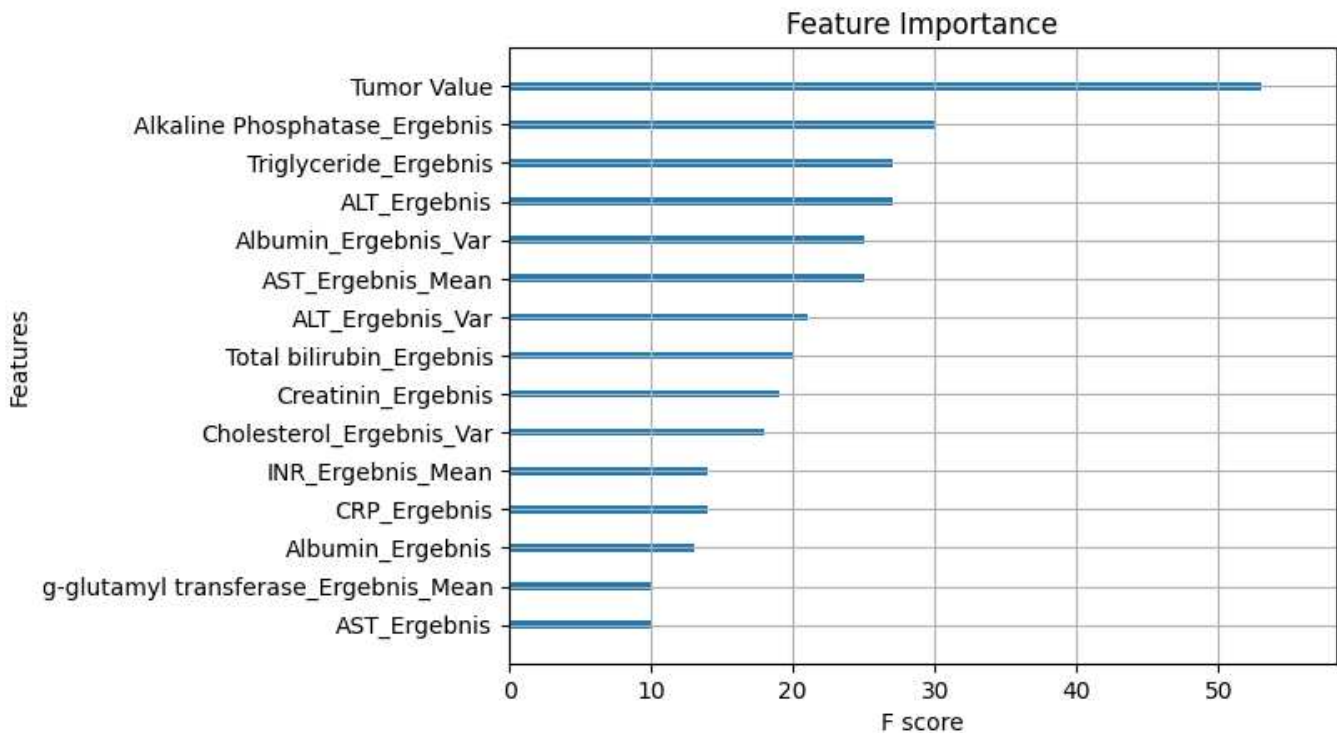


Figure 1: The importance of selected tabular features for TNM staging.

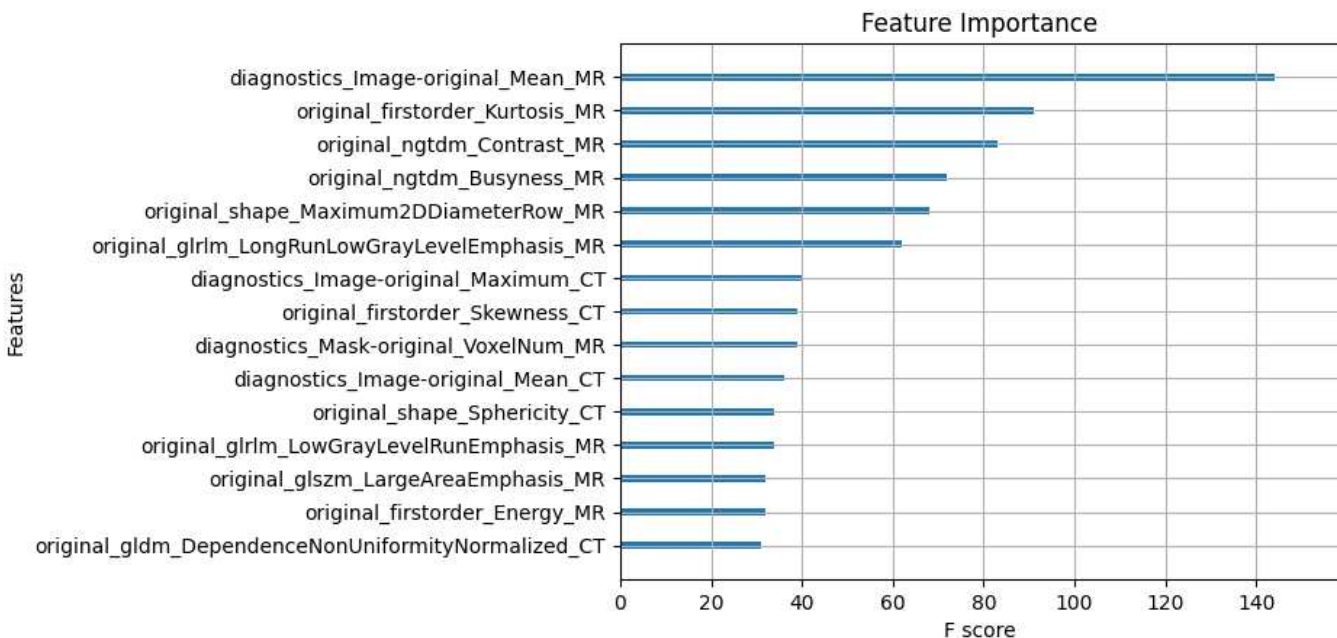


Figure 2: The importance of selected radiomics features for TNM staging.

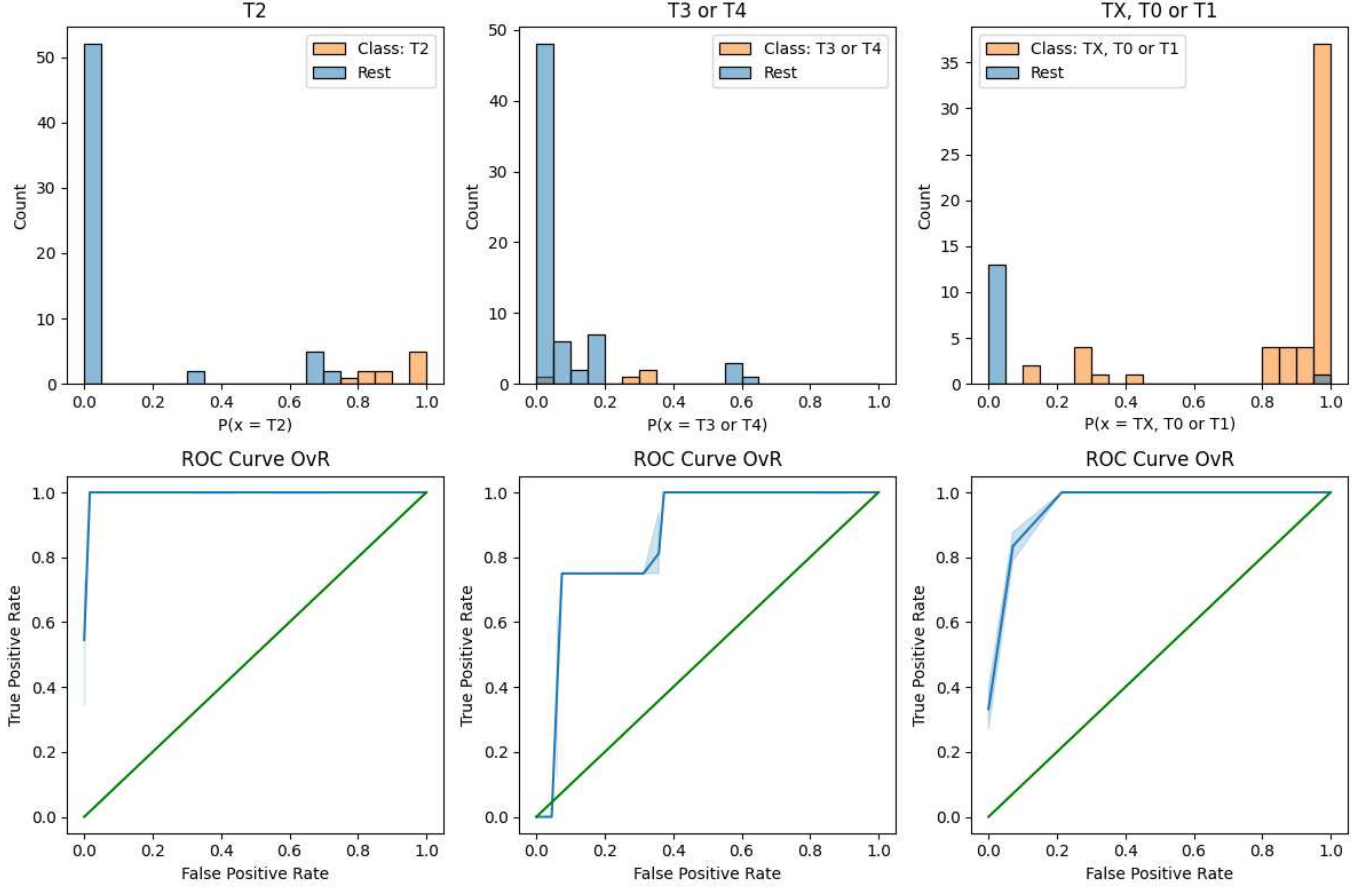


Figure 3: The probability distributions and the ROC curves (One vs Rest, OvR). In the first row are results of the probability distributions. The second row shows the corresponding ROC curves.

## 4 Conclusion

In this paper, we present a baseline model for handling multimodal clinical data classification using the state-of-the-art tabular data classifier. Our experiments demonstrate the effectiveness of combining tabular data and radiomics image features (from contrast-enhanced CT and MRI) for predicting TNM staging of HCC.

## 5 Acknowledgment

This project was funded by BMBF grant Q-HCC #grant number#.

### A Process of Filtering Feature Columns (Redcap data)

When filtering and selecting feature columns from the redcap dataset, the following principles were applied to ensure data simplicity, relevance, and model effectiveness:

#### A.1 Filter out features with less than 80% non-missing values

Columns with a non-missing value proportion below 80% were excluded to reduce noise and minimize the impact of missing data. This step ensures the retention of features with high information density, thereby improving data quality and model training efficiency.

## A.2 Filter out columns with identical values across all samples

Columns with the same value across all samples were removed because they contribute nothing to the classification task.

## A.3 Filter out data not closely related to the patient's cancer condition

Features unrelated to liver cancer classification, such as the following, were removed: Type of data collection (e.g., retrospective or prospective); Patient nationality; Categories of imaging diagnosis (e.g., whether a specific imaging study was performed); Examination dates; Label codes (e.g., laboratory study label codes); Patient consent information; Family health information.

## A.4 Filter intermediate scores used to calculate final stage ratings

For features associated with specific staging systems (e.g., BCLC staging with five stages), we retained only the final staging results and removed intermediate scores used for their calculation to avoid redundancy and reduce the potential for data overlap in model training.

## A.5 Filter out information related to subsequent treatment interventions

Data related to surgical stages or treatment interventions are primarily used for assessing treatment outcomes and are not essential for liver cancer classification task. Examples include: Specific surgical stages and procedures (e.g., liver segment resection information); Types and timing of follow-up treatments (e.g., whether specific drugs were administered).

## A.6 Handle features with high similarity rates

For columns with over 95% identical values, features not considered critical for classification (based on domain knowledge) or statistically insignificant to the target variable were filtered out.

## B The selected variables for the lab data

Table 3: The selected variables of lab data of the QHCC dataset.

Variable	Definition	Range of values
Hemoglobin	Protein in red blood cells that carries oxygen.	13.2–16.7 g/dL
Hematocrit	Proportion of red blood cells in the blood.	33.4–46.2%
Creatinine	Waste product from muscle metabolism, used to assess kidney function.	0.7–1.3 mg/dL
Sodium (Natrium)	Electrolyte important for fluid balance and nerve function.	136–145 mmol/L
ALT (Alaninaminotransferase)	Liver enzyme used to assess liver health.	7–40 U/L
Gamma-glutamyl transferase (GGT)	Enzyme involved in liver and bile duct function.	0–73 U/L
C-Reactive Protein (CRP)	Marker for inflammation in the body.	0–5 mg/dL
Total Bilirubin	Breakdown product of hemoglobin, assesses liver function.	0.2–1.0 mg/dL
Alkaline Phosphatase (ALP)	Enzyme related to bile ducts; also linked to bone health.	40–130 U/L
Aspartate Aminotransferase (AST)	Enzyme found in liver and muscles, used to assess liver damage.	13–40 U/L
INR (International Normalized Ratio)	Standardized number for blood clotting time, based on prothrombin time.	0.9–1.15
Albumin	Main protein in blood plasma, maintains oncotic pressure and transports substances.	35–48 g/L
Cholesterol	Type of fat found in the blood, important for cell membranes and hormones.	<200 mg/dL
Triglycerides	Type of fat (lipid) found in the blood.	<150 mg/dL
Hemoglobin A1c (HbA1c)	Average blood glucose level over the past 2–3 months, used in diabetes monitoring.	4–5.6% (normal) 5.7–6.4% (pre-diabetes) >6.5% (diabetes)
Alpha-fetoprotein (AFP)	Protein produced by the liver; elevated in liver diseases and certain cancers.	0–8.1 ng/mL
Direct Bilirubin	Conjugated bilirubin, measures liver's ability to excrete waste.	0.0–0.3 mg/dL
Ferritin	Protein that stores iron, used to assess iron levels.	26–388 ng/mL

## References

Julius Balogh, David Victor III, Emad H Asham, Sherilyn Gordon Burroughs, Maha Boktour, Ashish Saharia, Xian Li, R Mark Ghobrial, and Howard P Monsour Jr. Hepatocellular carcinoma: a review. *Journal of hepatocellular carcinoma*, pages 41–53, 2016.

Tiffany Hennedige and Sudhakar Kundapur Venkatesh. Imaging of hepatocellular carcinoma: diagnosis, staging and treatment monitoring. *Cancer Imaging*, 12(3):530, 2013.

Swapna Abhyankar, Dina Demner-Fushman, and Clement J McDonald. Standardizing clinical laboratory data for secondary use. *Journal of biomedical informatics*, 45(4):642–650, 2012.

Emily F Patridge and Tania P Bardyn. Research electronic data capture (redcap). *Journal of the Medical Library Association: JMLA*, 106(1):142, 2018.

Tian-yi Xia, Zheng-hao Zhou, Xiang-pan Meng, Jun-hao Zha, Qian Yu, Wei-lang Wang, Yang Song, Yuan-cheng Wang, Tian-yu Tang, Jun Xu, et al. Predicting microvascular invasion in hepatocellular carcinoma using ct-based radiomics model. *Radiology*, 307(4):e222729, 2023.

Somasundaram Subramaniam, Robin K Kelley, and Alan P Venook. A review of hepatocellular carcinoma (hcc) staging systems. *Chinese clinical oncology*, 2(4):33–33, 2013.

Joost JM Van Griethuysen, Andriy Fedorov, Chintan Parmar, Ahmed Hosny, Nicole Aucoin, Vivek Narayan, Regina GH Beets-Tan, Jean-Christophe Fillion-Robin, Steve Pieper, and Hugo JW Aerts. Computational radiomics system to decode the radiographic phenotype. *Cancer research*, 77(21):e104–e107, 2017.

Claude Elwood Shannon. A mathematical theory of communication. *The Bell system technical journal*, 27(3):379–423, 1948.

F. Pedregosa, G. Varoquaux, A. Gramfort, V. Michel, B. Thirion, O. Grisel, M. Blondel, P. Prettenhofer, R. Weiss, V. Dubourg, J. Vanderplas, A. Passos, D. Cournapeau, M. Brucher, M. Perrot, and E. Duchesnay. Scikit-learn: Machine learning in Python. *Journal of Machine Learning Research*, 12:2825–2830, 2011.

Isabelle Guyon, Jason Weston, Stephen Barnhill, and Vladimir Vapnik. Gene selection for cancer classification using support vector machines. *Machine learning*, 46:389–422, 2002.

Tianqi Chen and Carlos Guestrin. Xgboost: A scalable tree boosting system. In *Proceedings of the 22nd acm sigkdd international conference on knowledge discovery and data mining*, pages 785–794, 2016.

Duncan McElfresh, Sujay Khandagale, Jonathan Valverde, Vishak Prasad C, Ganesh Ramakrishnan, Micah Goldblum, and Colin White. When do neural nets outperform boosted trees on tabular data? *Advances in Neural Information Processing Systems*, 36, 2024.